



Characteristics of cubic MgZnO thin films grown by radio frequency reaction magnetron co-sputtering

S. Han^{a,b}, D.Z. Shen^a, J.Y. Zhang^{a,*}, Y.M. Zhao^a, D.Y. Jiang^a, Z.G. Ju^a, D.X. Zhao^a, B. Yao^a

^a Key Laboratory of Excited State Processes, Changchun Institute of Optics, Fine Mechanics and Physics, Chinese Academy of Sciences, 16 East Nan-Hu Road, Open Economic Zone, Chang chun 130033, People's Republic of China

^b Graduate School of the Chinese Academy of Sciences, Beijing 10039, People's Republic of China

ARTICLE INFO

Article history:

Received 24 January 2009

Received in revised form 7 June 2009

Accepted 12 June 2009

Available online 21 June 2009

PACS:

61.66. Dk

61.82.Fk

67.25.dp

Keywords:

MgZnO thin film

rf reaction magnetron co-sputtering

ABSTRACT

Cubic MgZnO thin films were prepared on fused quartz substrate by radio frequency (rf) reaction magnetron co-sputtering technique, and composition modulation of cubic MgZnO films could be accomplished by changing rf power on Zn metal target. During growth process crystal quality of our MgZnO films can be improved by increasing the ratio of O₂/Ar. Unlike reported growth of (1 1 1) plane cubic MgZnO films, our cubic MgZnO films show (2 0 0) plane growth properties. This phenomenon was assigned to a preferred selection growth characteristic of MgZnO on non-crystalline quartz substrate. Band gaps of cubic MgZnO films calculated by empirical formula are different from that obtained in the absorption spectrum. It is suggested that parts of Mg do not contribute to the band gaps of Mg_xZn_{1-x}O thin films.

© 2009 Elsevier B.V. All rights reserved.

1. Introduction

ZnO has attracted much attention because of its potential applications on optoelectronic devices in ultraviolet (UV) spectral region. Recently MgZnO also gained increasing interest due to the same fundamental material advantages as those found in pure ZnO, moreover its band gap can be tuned from 3.3 to 7.8 eV by varying the Mg composition which extend its use from UV-A (320–400 nm) to UV-B (280–320 nm) and UV-C (200–280 nm) regions. The wide sensing range is expected to enable MgZnO UV detectors to be used in many fields, such as solar UV radiation monitoring, ultra-high temperature flame detection and air-borne missile warning systems [1–4].

As well known, MgZnO alloys have two different crystal structures that are varied with Mg composition, i.e., the hexagonal phase (the ZnO-like wurtzite structure) with low Mg composition (<0.33) [5], and the cubic phase (the MgO-like NaCl structure) with high Mg composition (≥0.51) [6]. Both of the two structural MgZnO films have been grown by a variety of techniques, such as pulse laser deposition (PLD) [7–9], metal-organic chemical vapour deposition (MOCVD) [10,11], rf magnetron sputtering [12–17] and molecular beam epitaxy (MBE) [18,19]. Recently several reports

have been focused on the growth and characteristic study of cubic MgZnO for its applications in UV-C (200–280 nm) regions. The negative thermo-optical coefficient in cubic MgZnO thin films have been studied by Zhou and Shen [20], Narayan et al. have studied the characteristic of cubic MgZnO heterostructure grown on Spinel/TiN/Si(1 0 0) by PLD [21]. However, characteristics of cubic MgZnO thin films grown by rf magnetron reaction co-sputtering technique are rarely reported.

So in this work, the cubic Mg_xZn_{1-x}O thin films were prepared by rf magnetron reaction co-sputtering technique with Mg and Zn metal targets, respectively. When MgZnO films were prepared by rf magnetron reaction co-sputtering technique, Mg, Zn and O atoms reached the substrate separately, MgZnO films were formed through reaction between Mg, Zn and O atoms, so crystal quality of deposited Mg_xZn_{1-x}O films would be better than that of films by rf magnetron sputtering with chinaware target. And also convenient adjustment of Mg concentration in MgZnO films could be accomplished by changing ratio of rf powers on Mg and Zn metal targets. Therefore, by this technique it is expected that we can get high quality MgZnO film and convenient composition modulation. Meanwhile, structural and optical properties of cubic MgZnO films were studied.

2. Experimental

Mg_xZn_{1-x}O thin films were grown on quartz substrate using rf magnetron sputtering technique. The targets are a Mg (99.99%) metal target and a Zn (99.99%) metal

* Corresponding author. Tel.: +86 4316176322; fax: +86 4315682964.
E-mail address: zhangjy53@yahoo.com.cn (J.Y. Zhang).

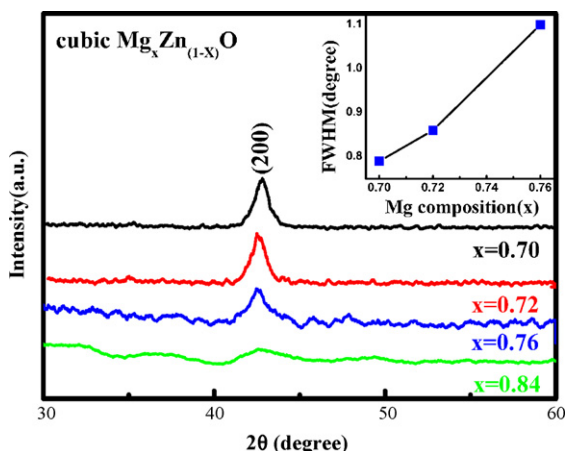


Fig. 1. XRD spectra of $\text{Mg}_x\text{Zn}_{1-x}\text{O}$ films grown on quartz substrates ($0.70 \leq x \leq 0.84$), XRD spectra of ZnO is given above as reference. The insert is the FWHM of MgZnO films as compositions Mg .

target placing at two different target seats. There are two electrodes installed on the two metal targets, respectively, which can be used to adjust the ratio of Mg/Zn by changing the ratio of rf powers. The distances between substrate and two targets are both 7.5 cm, and the substrate is not parallel to two targets. The $\text{Mg}_x\text{Zn}_{1-x}\text{O}$ films were deposited in a reactive gas ambient of $\text{Ar}:\text{O}_2$ (30:30) at 2.3 Pa sputtering pressure. In order to grow $\text{Mg}_x\text{Zn}_{1-x}\text{O}$ films with high Mg concentration, we set the applied rf power of Mg metal target at 130 W, but change the applied rf power of Zn metal target from 85 to 70 W. All the depositions were done with the substrate temperature of 600 °C.

The phase and crystallographic orientation of $\text{Mg}_x\text{Zn}_{1-x}\text{O}$ films were characterized by using an X-ray diffraction (XRD) technique. The composition of $\text{Mg}_x\text{Zn}_{1-x}\text{O}$ films is derived from energy-dispersive X-ray (EDX). Scanning electron microscope (SEM) was utilized to study the surface morphology of the samples. The transmission and absorption spectra were measured by UV–vis spectroscopy.

3. Results and discussions

Fig. 1 shows XRD patterns of as-grown $\text{Mg}_x\text{Zn}_{1-x}\text{O}$ thin films with different Mg content on quartz substrates. It can be seen that all $\text{Mg}_x\text{Zn}_{1-x}\text{O}$ films exhibit single rock-salt cubic structure $x \geq 0.70$ and only (200) diffraction peak can be observed around 42°. The insert shows the full width at half maximum (FWHM) value of (200) diffraction peak for $\text{Mg}_x\text{Zn}_{1-x}\text{O}$ films, from which the FWHM value of $\text{Mg}_{0.7}\text{Zn}_{0.3}\text{O}$ is 0.79°, and the FWHM value of cubic structure $\text{Mg}_x\text{Zn}_{1-x}\text{O}$ films increased with the increase of Mg composition, which indicates that crystal quality of the cubic structure $\text{Mg}_x\text{Zn}_{1-x}\text{O}$ films become worse with increasing Mg composition. According to previous report; the stress may be the main reason for this trend in ZnO [22]. In our case, $\text{Mg}_x\text{Zn}_{1-x}\text{O}$ films were made by sputter deposition on amorphous substrate at 600 °C, the stress induced by thermal mismatch would be one possible reason for above abnormally experimental results. Because the thermal expansion coefficient of ZnO crystal is $2.9 \times 10^{-6}/^\circ\text{C}$ smaller than $12.8 \times 10^{-6}/^\circ\text{C}$ of MgO crystal, the thermal expansion coefficient of $\text{Mg}_x\text{Zn}_{1-x}\text{O}$ would be increased with Mg composition. Meanwhile, the thermal expansion coefficient of quartz is just $5.7 \times 10^{-7}/^\circ\text{C}$, about one order of magnitude smaller than ZnO and MgO crystals, when Mg content of cubic $\text{Mg}_x\text{Zn}_{1-x}\text{O}$ increased, the stress induced by thermal mismatch between cubic $\text{Mg}_x\text{Zn}_{1-x}\text{O}$ and quartz substrate increased. So when Mg composition of $\text{Mg}_x\text{Zn}_{1-x}\text{O}$ is around 80%, crystal quality of $\text{Mg}_x\text{Zn}_{1-x}\text{O}$ films is clearly damaged.

As shown in Fig. 1, the MgZnO films exhibited (200) plane of cubic structure, rather than the (111) plane. Usually, MgZnO films exhibit cubic (111) plane on single crystal substrates like Al_2O_3 and $\text{Si}(111)$ [13–19], due to the cubic MgZnO films would grow along substrate's orientation. But in our case, cubic MgZnO

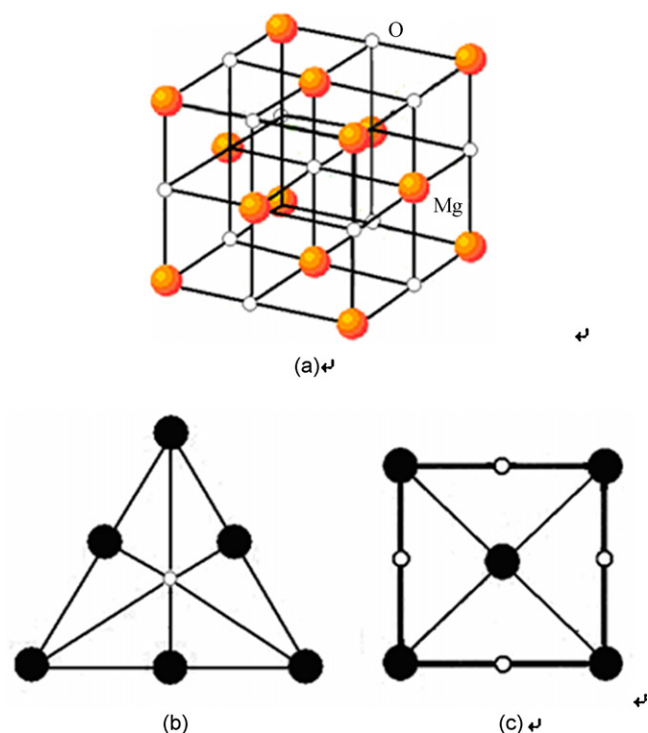


Fig. 2. (a) Schematic diagram of MgO crystal structure. (b) and (c) two planes of MgO crystal structure: (b) (111) plane (c) (002) plane.

films were deposited on non-crystalline substrate, therefore, they would grow in their own selective orientation. Brief description of the growth process have been given as follows: For non-polar cubic crystal, atom density of (111) plane is larger than that of (110) and (100) plane and crystal-plane distance of (111) plane is shortest. So vertical growth rate of (111) plane is the lowest, and the crystal face will be enveloped by (111) plane. But for compound semiconductor crystal like cubic MgO , rock-salt structure of which is showed in Fig. 2(a), there are two kinds of (200) planes and (111) planes, showed in Fig. 2(b) and (c). Because of much stronger ionic bond interaction between Mg ions and O ions, vertical growth rates of both (111) and (200) plane are increased. But atom density of (200) plane is smaller than that of (111) plane, and crystal-plane distance of (200) plane is larger than that of (111) plane, so effect of ionic bond interaction on (200) plane is weaker than that on (111) plane, which introduce lower vertical growth rate of (200) plane than (111) plane. So horizontal growth rate of (200) plane is higher. When crystal grows up, it would eat out contiguous crystal planes with lower horizontal growth rate. So in our case cubic $\text{Mg}_x\text{Zn}_{1-x}\text{O}$ ($x \geq 0.70$) films would grow along [200] preferred orientation, and it showed (200) plane of cubic $\text{Mg}_x\text{Zn}_{1-x}\text{O}$.

Fig. 3 shows the EDX spectrum of as-grown cubic MgZnO films on quartz substrate. There are only Mg , Zn and O elements except Si and O elements of substrate. The inset of Fig. 3 shows the ratio of Mg/Zn of $\text{Mg}_x\text{Zn}_{1-x}\text{O}$ films with different rf power on Zn metal target. It can be seen from the inset that Mg composition (x) would increase with the decrease of rf power on Zn metal target. That is to say, the adjustment of Mg composition of cubic $\text{Mg}_x\text{Zn}_{1-x}\text{O}$ films can be obtained by varying the rf power on Zn metal target.

Fig. 4 shows the UV–vis absorption spectrum of as-grown cubic $\text{Mg}_x\text{Zn}_{1-x}\text{O}$ films. It is found that the absorption edge of MgZnO thin film shifts to short wavelength with increasing Mg composition. Band gaps of $\text{Mg}_x\text{Zn}_{1-x}\text{O}$ films derived from a plot of $(\alpha h\nu)^2$ as a function of photon energy $h\nu$ are shown in the inset of Fig. 4. The absorption efficient (α) is obtained from the absorption spec-

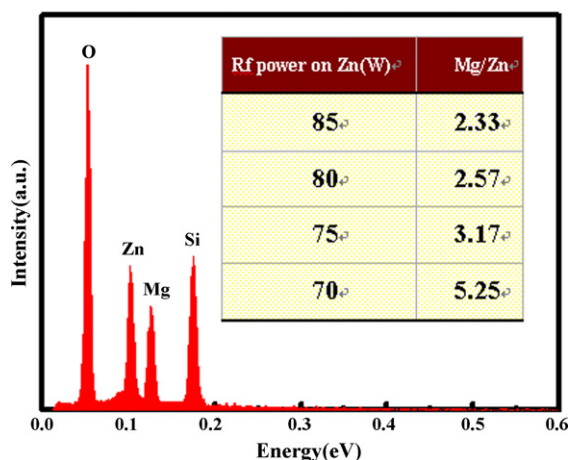


Fig. 3. Typical EDX spectrum of cubic $\text{Mg}_x\text{Zn}_{1-x}\text{O}$ films.

tra. The band gaps of the cubic $\text{Mg}_x\text{Zn}_{1-x}\text{O}$ films are 5.37, 5.47, 5.73 and 6.02 eV for the x value of 0.70, 0.72, 0.76, and 0.84, respectively. However, according to the results of EDX and the given equation ($E_g = 3.02 + 4.03x$) [23], the calculated band gaps of $\text{Mg}_x\text{Zn}_{1-x}\text{O}$ films (5.84, 5.92, 6.08 and 6.41 eV) with Mg compositions x (0.70, 0.72, 0.76, and 0.84) are clearly larger than that of experimental result in Fig. 4. This reason can be attributed to surplus Mg that cannot go into the MgZnO crystal lattice. It is known that the precipitate nanograin with a higher Mg concentration and the host with a higher Zn concentration coexisted in $\text{Mg}_x\text{Zn}_{1-x}\text{O}$ film have been approved [24]. Therefore, we consider our MgZnO films exited the similar structure; some Mg radicals may be in the form of clusters or other forms in the interfaces of crystal grains, which does not contribute to the absorption spectrum. So band-gaps values derived from absorption spectra are smaller than that calculated from the EDX data. In our case, cubic $\text{Mg}_x\text{Zn}_{1-x}\text{O}$ films were deposited under anoxic environment, which restricts binding of O and Mg atoms, so during deposition process anoxic environment may be one important factor for above phenomenon.

In order to confirm our surmise, we increased flow ratio of O_2/Ar during growth of $\text{Mg}_x\text{Zn}_{1-x}\text{O}$ films; Fig. 5 shows XRD spectra of as-grown MgZnO films with the ratio of O_2/Ar 1:1 and 2:1. The diffraction peaks show obvious shift to large angle side with the increasing of the ratio of O_2/Ar . It shows clearly that more oxygen can make more fully reactions between Mg atoms and O atoms, which will increase Mg composition of MgZnO films. This result shows that we can effectively increase the ratio of Mg/Zn of MgZnO

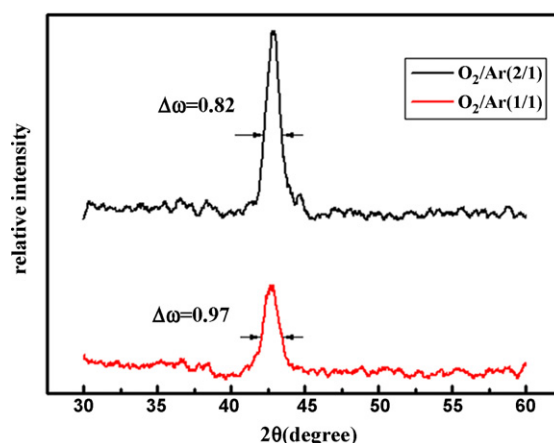


Fig. 5. XRD of as-grown $\text{Mg}_x\text{Zn}_{1-x}\text{O}$ films with O_2/Ar of 1/1 and 1/2.

films and their band gaps with extra oxygen. Through gauss fitting, we can get that full width at half maximum (FWHM) values of (200) rocking curves decreased from 0.97 to 0.82 with increased ratio of O_2/Ar , that is to say, crystal quality of films could be improved obviously by increasing the ratio of O_2/Ar .

4. Conclusion

Cubic (200) MgZnO films have been prepared by two-source (Zn and Mg) rf magnetron reaction co-sputtering technique. By this method, crystal quality of MgZnO films is expected to be improved, FWHM of $\text{Mg}_{0.7}\text{Zn}_{0.3}\text{O}$ is 0.79° , and also we achieved the modulation of composition and band gap of cubic MgZnO films by varying the sputtering power on Zn metal target. By increasing the ratio of Mg/Zn and changing flow ratio of O_2/Ar , it could make effective increasing Mg composition and the band gaps of cubic MgZnO films.

Acknowledgements

This work is supported by the Key Project of National Natural Science Foundation of China under Grant No.50532050, the “973” program under Grant Nos.2008CB317105 and 2006CB604906, the Knowledge Innovation Program of the Chinese Academy of Sciences, Grant No.KJJCX3.SYW.W01.

References

- [1] D.H. Zhang, D.E. Brodie, *Thin Solid Films* 238 (1994) 95.
- [2] Y. Takahashi, M. Kanamori, A. Kondoh, H. Minoura, Y. Ohya, *Jpn. J. Appl. Phys. Part 1* 33 (1994) 6611.
- [3] S.A. Studenikin, N. Golego, M. Cocivera, *J. Appl. Phys.* 87 (2000) 2413.
- [4] P. Sharma, A. Mansingh, K. Sreenivas, *Appl. Phys. Lett.* 80 (2002) 553.
- [5] S. Choopun, R.D.a.W. Vispute, R.P. Yang, T. Sharma, Venkatesan, *Appl. Phys. Lett.* 80 (2002) 94.
- [6] N.B. Chen, H.Z. Wu, D.J. Qiu, T.N. Xu, J. Chen, W.Z. Shen, *J. Phys. Condens. Mat.* 16 (2004) 2973.
- [7] Z. Vashaei, T. Minegishi, H. Suzuki, T. Hanada, M.W. Cho, T. Yao, A. Setiawan, *J. Appl. Phys.* 98 (2005) 054911.
- [8] A.K. Sharma, J. Narayan, J.F. Muth, C.W. Teng, C. Jin, A. Kvit, R.M. Kolbas, O.W. Holland, *Appl. Phys. Lett.* 75 (1999) 21.
- [9] J. Narayan, A.K. Sharma, A. Kvit, C. Jin, J.F. MO, W. Holland, *Solid State Commun.* 121 (2002) 9.
- [10] B.P. Zhang, N.T. Binh, K. Wakatsuki, C.Y. Liu, Y. Segawa, N. Usami, *Appl. Phys. Lett.* 86 (2005) 032105.
- [11] X. Dong, B.L. Zhang, X.P. Li, W. Zhao, X.C. Xia, H.C. Zhu, G.T. Du, *J. Phys. D: Appl. Phys.* 40 (2007) 7298.
- [12] Sanjeev Kumar, VinayGupte, K. Sreenivas, *J. Phys. Condens. Mat.* 18 (2006) 3343.
- [13] T. Minemoto, T. Negamib, S. Nishiwaki, H. Takakura, Y. Hamakawa, *Thin Solid Films* 372 (2000) 173–176.
- [14] C.-H. Choi, S.-H. Kim, *J. Cryst. Growth* 283 (2005) 170.
- [15] S.W. Kang, Y.Y. Kim, C.H. Ahn, S.K. Mohanta, H.K. Cho, *J. Mater. Sci.: Mater. Electron.* 19 (2008) 755–759.

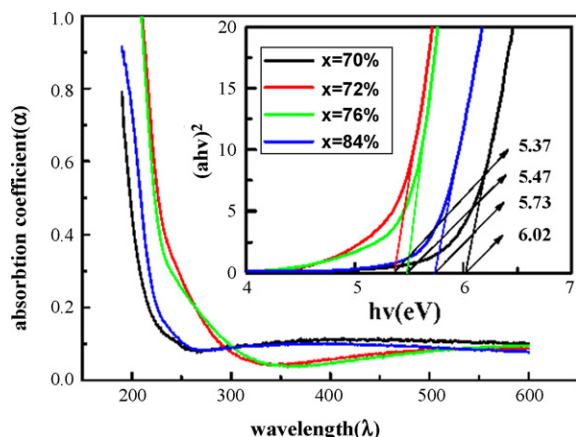


Fig. 4. UV–vis absorption spectrum of $\text{Mg}_x\text{Zn}_{1-x}\text{O}$ thin films ($0.70 \leq x \leq 0.84$) grown on quartz substrates.

- [16] C.X. Cong, B. Yao, Q.J. Zhou, J.R. Chen, J. Phys. D: Appl. Phys. 41 (2008) 105303.
- [17] E.Y. Jung, S.G. Lee, S.H. Sohn, D.K. Lee, H.K. Kim, Appl. Phys. Lett. 86 (2005) 153503.
- [18] J. Chen, W.Z. Shen, Appl. Phys. Lett. 83 (2003) 11.
- [19] K. Koike, K. Hama, I. Nakashima, G.-y. Takada, K.-i. Ogata, S. Sasaa, M. Inoue, M. Yano, J. Cryst. Growth 278 (2005) 288–292.
- [20] H.P. Zhou, W.Z. Shen, Appl. Phys. Lett. 85 (2004) 17.
- [21] J. Narayan, A.K. Sharma, A. Kvit, C. Jin, J.F. Moth, O.W. Holland, Solid State Commun. 121 (2002) 9.
- [22] A. Cimpoeasa, N.M. van der Pers, Th.H. de Keyser, A. Venema, M.J. Vellekoop, Smart Mater. Struct. 744–750 (1996) 5.
- [23] J. Chen, W.Z. Shen, N.B. Chen, D. Jiu, H. ZWu, J. Phys. B: Condens. Mat. 15 (2003) L475.
- [24] I. Takeuchi, W. Yang, K.S. Chang, M.A. Aronova, T. Venkatesan, R.D. Vispute, L.A. Bendersky, J. Appl. Phys. 94 (2003) 7336.